frontiers in Cellular and Infection Microbiology

ORIGINAL RESEARCH
published: 16 August 2021
doi: 10.3389/fcimb.2021.700198

Development of an Antibiotic Resistance Breaker to Resensitize Drug-Resistant *Staphylococcus aureus*: *In Silico* and *In Vitro* Approach

Gopalakrishnan Thamilselvan[1], *Hema Bhagavathi Sarveswari*[1], *Sahana Vasudevan*[1], *Alex Stanley*[2], *Karthi Shanmugam*[1,2], *Pothiappan Vairaprakash*[3] *and Adline Princy Solomon*[1*]

[1] Quorum Sensing Laboratory, Centre of Research in Infectious Diseases, School of Chemical and Biotechnology, SASTRA Deemed to be University, Thanjavur, India, [2] Department of Bioinformatics, School of Chemical & Biotechnology, SASTRA Deemed to be University, Thanjavur, India, [3] Department of Chemistry, School of Chemical & Biotechnology, SASTRA Deemed to be University, Thanjavur, India

OPEN ACCESS

Edited by:
Sanhita Roy,
LV Prasad Eye Institute, India

Reviewed by:
Ziqing Deng,
Beijing Genomics Institute (BGI), China
Jacques Joubert,
University of the Western Cape, South Africa

***Correspondence:**
Adline Princy Solomon
adlineprinzy@sastra.ac.in

Specialty section:
This article was submitted to Clinical Microbiology, a section of the journal Frontiers in Cellular and Infection Microbiology

Received: 25 April 2021
Accepted: 20 July 2021
Published: 16 August 2021

Citation:
Thamilselvan G, Sarveswari HB, Vasudevan S, Stanley A, Shanmugam K, Vairaprakash P and Solomon AP (2021) Development of an Antibiotic Resistance Breaker to Resensitize Drug-Resistant Staphylococcus aureus: In Silico and In Vitro Approach. Front. Cell. Infect. Microbiol. 11:700198. doi: 10.3389/fcimb.2021.700198

Efflux pumps are one of the predominant microbial resistant mechanisms leading to the development of multidrug resistance. In *Staphylococcus aureus*, overexpression of NorA protein enables the efflux of antibiotics belonging to the class of fluoroquinolones and, thus, makes *S. aureus* resistant. Hence, NorA efflux pumps are being extensively exploited as the potential drug target to evade bacterial resistance and resensitize bacteria to the existing antibiotics. Although several molecules are reported to inhibit NorA efflux pump effectively, boronic acid derivatives were shown to have promising NorA efflux pump inhibition. In this regard, the current study exploits 6-(3-phenylpropoxy) pyridine-3-boronic acid to further improve the activity and reduce cytotoxicity using the bioisostere approach, a classical medicinal chemistry concept. Using the SWISS-Bioisostere online tool, from the parent compound, 42 compounds were obtained upon the replacement of the boronic acid. The 42 compounds were docked with modeled NorA protein, and key molecular interactions of the prominent compounds were assessed. The top hit compounds were further analyzed for their drug-like properties using ADMET studies. The identified potent lead, 5-nitro-2-(3-phenylpropoxy)pyridine (5-NPPP), was synthesized, and *in vitro* efficacy studies have been proven to show enhanced efflux inhibition, thus acting as a potent antibiotic breaker to resensitize *S. aureus* without elucidating any cytotoxic effect to the host Hep-G2 cell lines.

Keywords: NorA, efflux Pump, *Staphylococcus aureus*, bioisostere, boron acid, antimicrobials

INTRODUCTION

Antibiotics are the first class of drugs that have been effective in treating many infections of clinical importance (Fernandes, 2006). However, the widespread usage and cross-reactivity of these antibiotics have enabled bacteria to gain resistance against most of the drugs through their evolutionary mechanisms (Tomoari et al., 2014). Consequently, treatment of bacterial infections is becoming a challenge due to the emergence of multidrug resistant organisms (MDROs) (Tugal et al., 2015). Among the MDROs is methicillin-resistant *Staphylococcus aureus* (MRSA), a major cause of hospital-acquired (nosocomial) and community-acquired infections (Hartmann et al., 2010). Also, the complexity increases in the treatment of MRSA with standard therapies as it exhibits resistance to the drugs of the latest resort such as tetracyclines, aminoglycosides, and fluoroquinolones (Marquez, 2005; Sabatini et al., 2012). MRSA exhibits a diversity of resistance mechanisms against antimicrobials that either reduce or prevent their transport into the cell or efflux them from the cell with multidrug resistant transporters (MDR pumps) (Sangwan et al., 2008). Among known resistance mechanisms, MDR pumps are transport proteins involved in the extrusion of toxins from the bacterial cells and show resistance to a wide range of antimicrobial compounds as well as host-derived microbicidal compounds thus enabling the bacteria to thrive in their ecological niche (Sun et al., 2014; Blair et al., 2015). To date, 14 MDR pumps have been described for *S. aureus*, including NorA, NorB, MedA, QacA/B, and Smr (Costa et al., 2013). The NorA efflux pump that belongs to the major facilitator superfamily (MFS) is a significant contributor to antibiotic resistance as it can expel a wide range of chemical probes, such as ethidium bromide (EtBr), acriflavine, quaternary amine compounds, fluoroquinolones, rhodamine-6-G, puromycin, and chloramphenicol (CHL), and confers resistance (Markham et al., 1999). Also, NorA shares sequence homology with other MDR pumps, which led to a hypothesis that it may possess a large hydrophobic binding pocket with a wide range of substrate specificity and so an attractive novel drug target for the identification of efflux pump inhibitors (EPIs) to fight against resistance (Neyfakh, 2002; Poole and Lomovskaya, 2006; Cloete R. et al., 2018). Several non-antibiotics such as reserpine, verapamil, flavones, isoflavones, porphyrin pheophorbide A, and acylated glycosides are reported to be NorA inhibitors that act as selective small-molecule modulators rather than clinical drug candidates (Schillaci et al., 2017). In this context, the efforts are focused on the design and synthesis of novel chemotypes, which could synergize with ciprofloxacin (CIP) against *norA* overexpressing *S. aureus* strains and impact on clinical relevance (Sabatini et al., 2011; Sabatini et al., 2013; Astolfi et al., 2017; Felicetti et al., 2017). Based on the recent study, chemicals with boronic acid entities are proven to be the potential inhibitors of the NorA efflux pump and reduce the antibiotic concentration fourfold (Fontaine et al., 2015). On a closer look to the synthesis protocol, the synthesis of chemicals having boron species requires the use of dangerous lithium reagents (Leermann et al., 2011), magnesium reagents (Clary et al., 2011), and more expensive palladium and iridium catalysts (Jiang et al., 2016). Several literary works also support the use of lithium, palladium, and iridium catalysts for the synthesis procedure (Sharp and Snieckus, 1985; Sharp et al., 1987; Zhdankin et al., 1999; Das et al., 2003; Billingsley and Buchwald, 2008; Hafner et al., 2016). To overcome the challenges of toxicity and high cost involved, the current work undertakes a classical medicinal chemistry approach of bioisostere replacement. Bioisosterism allows molecularly modifying the lead compound without compromising the drug target interaction, enhances the biological activity with improved pharmacokinetics, and reduces toxicity (Patani and LaVoie, 1996). In this regard, the current work aims to design new molecules from the reported lead compound by replacing the boronic acid moiety with a small molecule chemotype capable of restoring CIP activity on *S. aureus* strains by inhibition of NorA using SwissBioisostere (Wirth et al., 2013). This study combines systematically the interdisciplinary aspect of bioinformatics, medicinal chemistry, and microbiological studies to design and validate a promising NorA EPI.

MATERIALS AND METHODS

NorA Efflux Pump: 3D-Structure Prediction and Quality Assessment

The efflux pump, NorA, is a hydrophobic protein having 12 putative transmembrane domains. As the name suggests, the NorA efflux pump is used for the transport of fluoroquinolones, resulting in the limited efficacy of the antibiotic. As the experimentally determined 3D structure of the NorA efflux pump is not yet publicly available, we attempted to predict its structure using a theoretical approach. The primary amino acid sequence of NorA of *S. aureus* (accession number: Q5HHX4) with 388 amino acids (42.324 Da) was downloaded from UniProtKB (www.uniprot.org). The 3D structure of the downloaded NorA sequence was predicted using the I-TASSER (Iterative Threading ASSEmbly Refinement) server (https://zhanglab.dcmb.med.umich.edu/I-TASSER/). I-Tasser is a hierarchical protocol for automated protein structure prediction. A detailed systematic approach is used to generate the atomic structure models through multiple thread alignments, iterative assembly simulations, and finally, atomic-level structure refinement. The I-TASSER output is the C-score, a confidence score for estimating the quality of predicted models. The C-score is typically in the range of [-5, 2], where a C-score of a higher value signifies a model with high confidence and *vice versa*. We obtained the C-score of model-1 = -0.13, model-2 = 0.43, model-3 = -0.26, model-4 = -3.01, and model 5 = -3.40 for the top 5 models obtained from I-TASSER. Based on the C-score, we have chosen model-2 for further quality assessments. The stereochemical quality of model-2 was further evaluated using the Ramachandran plot. The plot made between the phi and psi angles of model-2 showed that 98.2% of the residues are in the favored region, and 1.8% of the residues are in the disallowed region. Since the C-score and the stereochemistry of model-2 were good and acceptable, we have chosen them for further molecular docking studies.

Bioisosteric Replacement

Earlier studies reported that boronic species were found to inhibit the NorA efflux pump and potentiate ciprofloxacin activity (Fontaine et al., 2014). In the present study, we derived biologically equivalent replacements (bioisosteres) for the chosen parent chemotype, 6-(3-phenylpropoxy)pyridine-3-boronic acid, by replacing the boronic acid (-$B(OH)_2$) functional group with other equivalent bioisosteres using the SwissBioisostere (http://www.swissbioisostere.ch) web-server interface (Wirth et al., 2013). The SwissBioisostere database contains information on 21,29,355 data points, corresponding to ~5,586,482 unique replacements, which are mapped to their biological performance in biochemical assays. The biological performance corresponds to 1,948 molecular targets and 30 target classes. This allows bioisosteric modifications of boronic acid in 6-(3-phenylpropoxy)pyridine-3-boronic acid. The 2D structure of 6-(3-phenylpropoxyl)pyridine-3-boronic acid was drawn using MarvinSketch 6.2 embedded in the SwissBioisostere server. Using the "Fragment 1" window in the SwissBioisoster, the boronic acid functional group (-$B(OH)_2$) was kept intact, and the remaining part of the structure was grouped and labeled as the -R group and queried against the database. This search enables SwissBioisoster to identify biologically equivalent functional groups through the detection of matched molecular pair and mining bioactivity data in the ChEMBL database. It gives an output of an extensive overview of which replacements for the queried substructure (-$B(OH)_2$) have been observed in the database. There are 42 equivalent replacements for the boronic acid that were identified by the webserver. It also provides the observed frequency, activity difference distribution, success-based score, or chemical similarity between the fragments.

Ligand Preparation

The 2D structures of all the 42 bioisosteric replacements obtained through SwissBioisosters were drawn using MarvinSketch (v17) (https://chemaxon.com/products/marvin). Efficient and accurate 2D to 3D conversion is a key precursor to any computational analyses. We used the LigPrep module implemented in Schrodinger for preparing the ligands. LigPrep generates accurate energy minimized 3D molecular structures and eliminates mistakes in ligands to reduce downstream computational errors. All the 42 compounds were saved as a single sdf file and prepared using the LigPrep wizard. OPLS-2005 forcefield was used for energy minimizing and optimizing the structures. We did not expand tautomeric and ionization states and stereoisomers for the input structures, as it may influence the bioisosteric replacements.

Protein Preparation

Any successful structure-based modeling research demands an accurate starting structure. Hence, the 3D structure of NorA protein modeled using I-TASSER (model-2) was prepared using protein preparation wizard implemented in Schrodinger (Sastry et al., 2013). Our protein preparation briefly includes adding missing hydrogens, determining optimal protonation states for histidine residues, optimizing protein's hydrogen bonding network, and restraining energy minimization. The prepared protein was further used for molecular docking studies.

Binding Site Prediction and Receptor Grid Generation

The accuracy of any molecular docking studies depends on how precisely the binding sites are defined (Friesner et al., 2006). In the absence of an experimentally solved co-crystallized structure of NorA with known inhibitors, we used Schrodinger SiteMap for predicting the binding sites of the modeled NorA protein (model-2). The highest-ranked binding site (Sitecore = 1.119) was selected as the putative NorA binding site, and Ile23, Pro24, Leu26, Pro277, Phe 47, Arg98, Val144, Tyr225, and Gly348 were set as binding site residues. The selected binding site residues agree with some of those residues reported in previous studies (Kalia et al., 2012). The binding site for molecular docking was defined using the receptor grid generation wizard implemented in Schrodinger. The grid box was kept cantered on the binding site amino acids identified using Sitemap. The size of the box was set to default. We visually inspected and confirmed that all the key binding site amino acids are within the defined grid box.

Molecular Docking

Molecular docking study was carried out using the Glide XP (extra precision) algorithm implemented in Schrodinger. Glide XP reliably finds the correct binding modes and outperforms other docking programs in receiving lower RMS deviations from the native-crystallized structure. All the 42 ligands were docked onto the binding site of the modeled NorA protein. The docking results were analyzed based on the glide score and the binding interactions. The protein–ligand complex interactions were visualized using PyMOL (https://pymol.org/2/).

ADMET Predictions

Accurate prediction of ADMET properties before expensive experiments on preclinical and clinical studies is essential to reduce the failure of the drug in the later stages. We used Schrodinger QikProp for evaluating the drug-likeness of the identified lead molecules. QikProp predicts the widest variety of pharmaceutically relevant properties including AlogP, PSA, hepatotoxicity, CYPD26 inhibition, aqueous solubility, blood–brain barrier penetration, and human oral absorption, Initially, the newly generated lead molecules through bioisosteric replacements were filtered for Lipinski's rule of 5 (molecular weight ≤ 500 Da, lipophilicity ≤ 5, hydrogen bond donor ≤ 5, hydrogen bond acceptor ≤ 10). Those molecules that satisfied Lipinski's rule of 5 were further screened for Veber's rule (rotatable bonds < 10 Å and polar surface area < 140 Å). The most important ADMET descriptors were calculated for the molecules that satisfied Veber's rule (Lipinski et al., 2001; Shinzato et al., 2020).

Synthesis of the Selected Bioisostere, 5-Nitro-2-(3-Phenylpropoxy)Pyridine

5-Nitro-2-(3-phenylpropoxy)pyridine (5-NPPP) was synthesized by treating (3-bromopropyl)benzene with 5-

nitropyridin-2-ol in a basic medium provided by K_2CO_3 in acetonitrile solvent. The reaction was carried out at 80 °C for 2 h.

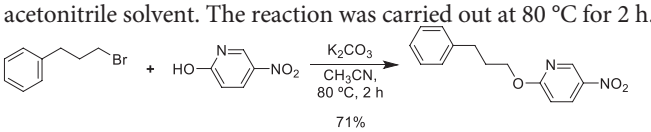

71%

In a typical synthesis, a mixture containing 5-nitorpyridin-2-ol (1.00 g, 7.14 mmol), (3-bromopropyl) benzene (1.71 g, 8.57 mmol, 1.31 mL), potassium carbonate (1.4 g, 10.1 mmol), and acetonitrile (5.0 mL) was stirred at 80 °C for 2 h. Then, the reaction mixture was filtered, and the filtrate was concentrated. The resulting mass was purified by column chromatography to obtain 5-NPPP as a yellow-colored solid (1.3 g, 71% yield). The compound was characterized by NMR spectroscopy. ^{1}H NMR (300 MHz, $CDCl_3$) δ 2.17 (qt, J = 7.5 Hz, 2H), 2.74 (t, J = 7.5 Hz, 2H), 4.02 (t, J = 7.5 Hz, 2H), 6.54 (d, J = 9.9 Hz, 1H), 7.18-7.34 (m, 5H), 8.06 (dd, J_1 = 9.9 Hz, J_2 = 3.0 Hz, 1H), 8.48 (d, J = 3.0 Hz, 1H); ^{13}C NMR (75 MHz, $CDCl_3$) δ 29.9, 32.6, 50.8, 119.6, 126.4, 128.2, 128.7, 130.5, 133.0, 139.3, 139.8, 161.4; ESI-MS obsd 259.1079, calcd 259.1077 [(M + H)$^+$,M = $C_{14}H_{14}N_2O_3$].

Bacterial Strains and Growth Conditions

S. aureus clinical isolates (*Sa*-P1987, *Sa*-P1920, *Sa*-AB459, *Sa*-P2003, *Sa*-Eye33, *Sa*-P2017, *Sa*-AB77, and *Sa*-P1995) were received from J.S.S Medical College, Mysore, and ATCC 29213, SA-1199B, and SA-1199 were used for the study. The *S. aureus* strains were retrieved from glycerol stocks and were maintained in Trypticase Soy Agar (TSA; HiMedia; Mumbai; India) at 37° C.

Chemicals and Antibiotics

Antibiotics (vancomycin (VAN), cefoxitin (CEF), norfloxacin (NOR), cephalexin (CEP), ciprofloxacin (CIP), CHL, azithromycin (AZI), cloxacillin (CLO), EtBr, and Verapamil) were purchased from Sigma-Aldrich Chemical Co. (St. Louis, MO). The stock solutions of antibiotics and inhibitors were prepared with sterile water. In the case of reserpine, dimethyl sulfoxide (DMSO) was used for the preparation of the initial stock solution and further diluted to desired concentrations with water or culture broth (Aeschlimann et al., 1999).

Resistance/Susceptible Profiling of Selected *S. aureus* Isolates

The antibiotic resistance/susceptibility assay was carried for both the standard and clinical isolates by the broth microdilution method according to CLSI guidelines (Wikler, 2006). The selected antibiotics, VAN (16 μg ml^{-1}), CEF (8 μg mL^{-1}), NOR (16 μg ml^{-1}), CEP (32 μg ml^{-1}), CIP (128 μg ml^{-1}), CHL (30 μg ml^{-1}), AZI (32 μg ml^{-1}), and CLO (128 μg ml^{-1}), were used for MIC determinations as interpreted in the susceptibility interpretive criteria reported in the appropriate CLSI tables.

Correlation of MDR With Overexpression of Efflux Pump, NorA

S. aureus clinical isolates grown overnight in TSB 37 °C were diluted to 100-fold in fresh TSB. The broth was incubated at 37 °C with shaking at 250 rpm for 3 h (OD_{600} of ∼0.6). RNA protect bacteria reagent (Qiagen) was added to the cell culture and left at room temperature for 30 min. Cell pellets were collected and lysed as described in the RNAprotect Bacteria Reagent Handbook (Lan et al., 2010). Total RNA was extracted by following the manufacturer's guidelines of the HiMedia RNA Extraction Kit (MB613). The integrity and purity of the extracted RNA were verified using agarose gel electrophoresis and NanoDrop (Thermo Scientific, Waltham, USA), respectively. Total RNA was converted to cDNA using the iScript™ cDNA Synthesis Kit using the manufacturer-recommended protocol. Relative quantification of NorA gene expression was performed with *gmk* (guanylate kinase) as the housekeeping gene, using the fast-real-time PCR system (Eppendorf, India) (**Table S1**). The resistance pattern of the selected strains was correlated with the cycle threshold (CT) of *norA* as it is inversely proportional to its expression level. The strain that showed the lowest CT value was scored for its overexpression of NorA and chosen for further study, and it was confirmed with the EtBr efflux assay (Schmittgen and Livak, 2008; Balasubramanian et al., 2020; Tinoush et al., 2020).

Determination of Minimum Inhibitory Concentration of 5-NPPP

The minimum inhibitory concentration (MIC) of the bioisostere, 5-NPPP, was determined against the *norA* overexpressed clinical isolate, *Sa*-P2003. The strain was grown at 37° C in Mueller–Hinton Broth and diluted until it reached a cell density of 2.9*10^8 CFU ml^{-1}. Varying concentrations of the 5-NPPP (1 to 1,000 μg mL^{-1}) were tested against the growth of the clinical isolate, *Sa*-P2003, and SA-1199B. After 24 h, the growth of the cells was recorded at 595 nm using a 96-well microtiter plate reader (BioRad i-Mark). The MIC of 5-NPPP is defined as the lowest concentration that inhibits the growth by ≥ 90% (for MIC_{90}) or ≥ 50% (for MIC_{50}) when compared to control (untreated) (Rodríguez-Tudela et al., 2003).

Determination of Minimum Effective Concentration of 5-NPPP

The overnight diluted bacterial suspension of *Sa*-P2003 and SA-1199B was plated in 96-well microtiter plates containing varying concentrations of 5-NPPP (0.5 to 0.125 μg ml^{-1}) and CIP (0.25–8 μg ml^{-1}). The culture condition was maintained at 24 h at 37 °C, and after 24 h, the growth inhibition was evaluated by measuring the OD_{595}. The untreated bacterial culture was taken as a negative control. The percentage inhibition of the combination and individual treatments of cultures were calculated to score minimum effective concentration (MEC). Furthermore, the 5-NPPP and CIP interaction was analyzed by fitting the data in a zero interaction potency (ZIP) model using the R-package synergy finder (https://bioconductor.org/packages/release/bioc/html/synergyfinder.html).

EtBr Efflux Assay

For the EtBr efflux assay, NorA overexpressing *Sa*-P2003 and *S. aureus* SA-1199B cultures as independent trials were suspended to an OD of 0.2 in buffer (50 mM NH_4Cl, 110 mM NaCl, 52 mM Tris base, 7 mM KCl, 0.4 mM Na_2HPO_4, and 0.2% glucose) with pH adjusted to 7.5. The cells were loaded with a dose of 10 μg ml^{-1}

EtBr as it does not exert any cytotoxic effect. Then, the EtBr-loaded cells were centrifuged at 12,000 rpm for 5 min, and then, pelletized cells were resuspended in EtBr-free PBS buffer with 0.4% glucose supplemented either with or without 5-NPPP (0.25 μg ml^{-1}). A known NorA inhibitor, verapamil (25 μg ml^{-1}), was used as a positive control. The real-time EtBr efflux from the cells was observed at every 5-min intervals for 30 min in triplicates. The intensity of fluorescence was measured at 530 nm for excitation and 600 nm for emission, respectively, using a Jasco FP-8200 spectrofluorometer (Jasco Corporations, Japan) (Brenwald et al., 1998).

Cytotoxicity Assays

Hep-G2 (human liver carcinoma) was purchased from NCCS, Pune and cultured in an RPMI medium at 37°C under 5% CO_2 supplemented with 10% fetal bovine serum (FBS), 100 U ml^{-1} penicillin, and 100 μg ml^{-1} streptomycin. The cell viability was assessed by the reduction of the dye, 3-(4,5-dimethylthiazol-2-yl)-2, 5-diphenyltetrazolium bromide to purple formazan crystals by mitochondrial succinate dehydrogenase enzyme in living cells. The cells were seeded into 96-well plates at a concentration of 10^4 cells/well and allowed to incubate for 24 h. Once the cells reached a subconfluent stage, then they were incubated with the bioisostere, 5-NPPP, at its 1XMIC, 10X, and 100X MIC for 48 h. After incubation, 10 μL of MTT (5 mg ml^{-1} in PBS) was added to the microtiter plate and was incubated for 4 h at 37° C. The MTT was removed, and 100 μL DMSO was added to each well to solubilize formazan crystals. Plates were incubated at 37° C for 20 min, and the absorbance was read at OD_{590}. Experiments were performed in triplicates, and the percentage cell viability was calculated (Kakhki et al., 2014).

Statistical Analysis

The results were expressed as mean ± SD. Statistical analysis was performed using the GraphPad Prism software version 8 (GraphPad Software Inc., San Diego, CA, United States). Significance was checked with the Dunnett *t*-test for multiple comparisons and paired Student's *t*-test ($p \leq 0.05$) (Balasubramanian et al., 2020).

RESULTS

Structural Prediction and High Throughput Virtual Screening of NorA Inhibitors Using the Bio-Isosteric Approach

The 3D structure of *S. aureus (strain COL)* Quinolone resistance protein NorA sequence (PDB Accession no: Q5HHX4) (**Figure 1**) was modeled and validated by a Ramachandran plot. The molecular interactions of the generated 42 compounds with the modeled NorA protein were analyzed using molecular docking. The docked complexes were further subjected for binding free energy calculations using Molecular mechanics/Generalised Born Surface Area (MMGBSA) (**Table 1**), and the higher the negative value the stronger the interaction and the higher the binding affinity. Out of these 42 compounds, 19 compounds displayed binding energies that ranged between −6.07 and −7.2 kcal/mol indicating a greater potential for the ligand to bind to NorA. This greater binding potential exertion was followed by another 20 compounds that showed binding energies from −4.0 to −5.9 kcal/mol. MMGBSA calculations of the receptor–ligand complex showed that the complexes formed between the NorA and ligands are highly stable (**Table 1**). Investigation of the interaction between 5-NPPP was analyzed based on the docking scores. The ligand 5-NPPP was positioned within the transmembrane alpha helixes of the modeled NorA. The parent chemotype binds within hydrophobic cleft having residues Ile19A, Phe47A, and Phe16A, while the 5-NPPP binds with Ile19A, Phe47A, Phe16A, and Phe140A (**Figure 2**).

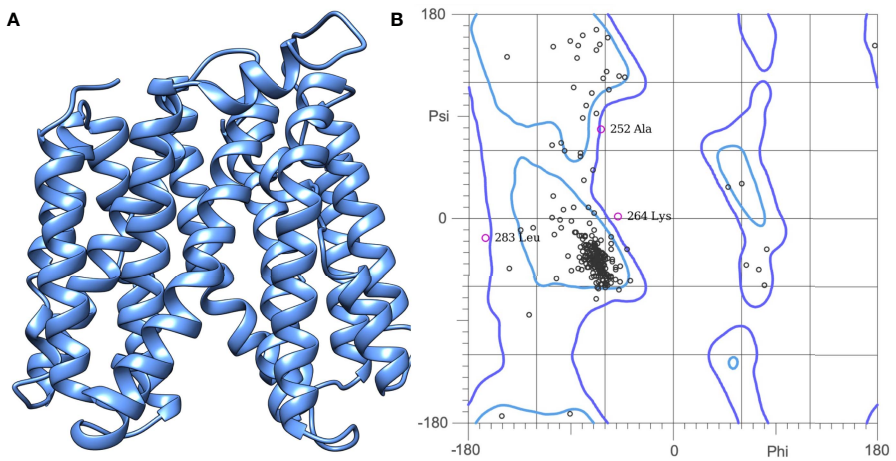

FIGURE 1 | **(A)** Construction of the NorA efflux pump model: A three-dimensional model of NorA was generated using I-TASSER. The best scoring model (C-score = 0.43; TM Score = 0.70 ± 0.12) was visualized using UCSF Chimera. **(B)** Quality prediction of modeled NorA protein using the Ramachandran plot. The structure of NorA protein is found to span in the regions of beta-sheets and right-handed alpha helix. Phi and Psi represent the torsion angles.

TABLE 1 | Identification of lead compound through screening of small molecules based on docking and activity scores.

S. No.	Compound	Activity	Frequency	Score	Better	Equal	Worse	R group Distance	Docking Score	MMGbsa
1.	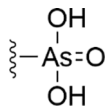		36	0.83	27	5	4	2.56	NIL	NIL
2.			19	0.31	4	1	14	7.99	-6.927	-47.14
3.	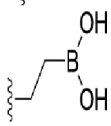		12	0.9	11	1	0	11.61	-6.928	-53.44
4.	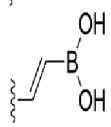		11	0.6	6	1	4	11.95	-6.952	-40.01
5.	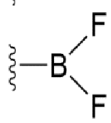		10	0.73	1	7	2	7.02	-6.308	-40.22
6.	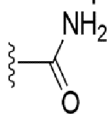		7	0.35	2	0	5	3.51	-6.654	-32.41
7.	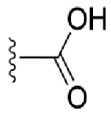		6	0.75	3	2	1	4.61	-4.946	-35.87
8.			5	0.5	2	0	3	8.77	-4.258	-42.78
9.			5	0.74	2	2	1	12.84	-5.913	-42.31
10.	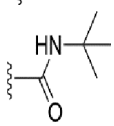		5	0.17	0	0	5	7.01	-4.201	-40.56
11.			4	0.83	4	0	0	12.36	-4.894	-38.78
12.			4	0.65	2	1	1	10.66	NIL	NIL
13.	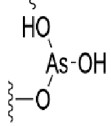		3	0.82	2	1	0	10.66	-4.159	-36.9
14.			3	0.82	2	1	0	10.66	-4.786	-40.28
15.	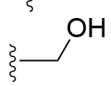		2	0.74	2	0	0	4.91	-5.253	-46.04
16.	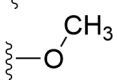		2	0.61	0	1	1	10.51	-6.07	-46.02
17.	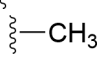		2	0.77	1	1	0	9.46	-4.775	-39.68
18.			2	0.78	1	1	0	10.67	-5.117	-46.1
19.	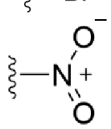		2	0.78	1	1	0	8.11	-4.52	-39.36
20.			2	0.79	1	1	0	10.66	-6.183	-41.64

(Continued)

TABLE 1 | Continued

S. No.	Compound	Activity	Frequency	Score	Better	Equal	Worse	R group Distance	Docking Score	MMGbsa
21.	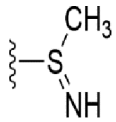		2	0.5	1	0	1	5.17	-5.868	-50.7
22.	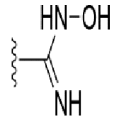		2	0.76	2	0	0	7.45	-5.844	-32.88
23.	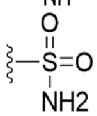		2	0.5	1	0	1	5.34	-6.205	-46.46
24.	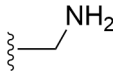		2	0.76	2	0	0	4.49	-4.861	-42.66
25.	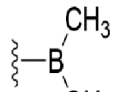		1	0.7	1	0	0	1.16	-5.915	-42.9
26.	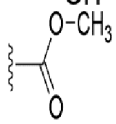		1	0.7	1	0	0	6.22	-5.807	-45.08
27.	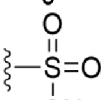		1	0.7	1	0	0	4.44	-5.627	-45.91
28.	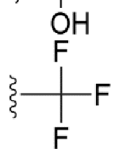		1	0.7	0	1	0	8.52	-6.949	-41.68
29.	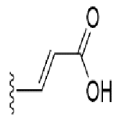		1	0.69	0	1	0	11.75	-6.074	-60.36
30.	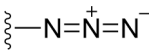		1	0.7	1	0	0	11.19	-5.849	-41.46
31.	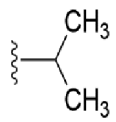		1	0.7	1	0	0	9.62	-6.634	-40.91
32.	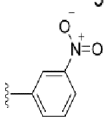		1	0.7	1	0	0	11.65	-6.923	-52.42
33.	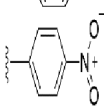		1	0.7	1	0	0	11.46	-6.105	-46.13
34.	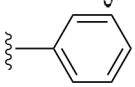		1	0.7	1	0	0	11.08	-6.728	-49.33
35.	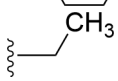		1	0.7	0	1	0	8.95	-4.417	-37.35

(Continued)

TABLE 1 | Continued

S. No.	Compound	Activity	Frequency	Score	Better	Equal	Worse	R group Distance	Docking Score	MMGbsa
36.	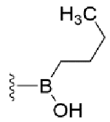		1	0.3	0	0	1	4.11	-6.784	-50.55
37.	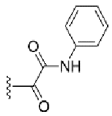		1	0.34	0	0	1	9.88	-6.447	-47.61
38.	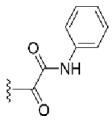		1	0.3	0	0	1	10.15	-6.685	-53.01
39.	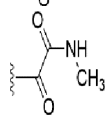		1	0.3	0	0	1	9.05	-6.075	-48.34
40.	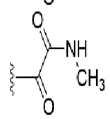		1	0.3	0	0	1	10.31	-7.217	-56.86
41.	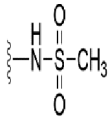		1	0.3	0	0	1	11.75	-6.669	-50.47
42.	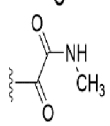		1	0.3	0	0	1	4.94	-5.843	-52.35

Docking score found between the range –4.0 and –6.7 with MMGBSA scores between –35.0 and –49.3 as estimated binding energy. MMGBSA defines the strength of binding between the ligand and the receptor; a greater value relates to the stronger binding. The activity of the replaced molecules is shown as nonpotentiating (RED color), may either potentiate or decrease the activity (ORANGE color), or potentiates the activity of the drug (GREEN color).

Pharmacokinetic Assessment (ADMET)

The drug-likeness of the newly generated bioisosteres was analyzed by Lipinski's rule of 5. The majority of the compounds were below ALogP98, and 90% of the compounds have less hepatotoxicity. Twenty-four compounds displayed a good solubility, while the rest of the compounds had moderate solubility. In the case of adsorption and penetration, the majority of the generated compounds displayed potential for significant adsorption and penetration within a biological system. Overall, ADMET analysis revealed that 90% of the compounds generated in our study were more likely toward a potential drug (**Table 2**). Our interest molecule, 5-NPPP having an AlogP98 score of 3.418 and Pressure Swing Adsorption (PSA) of 46.42 was chosen. The presence of the functional (-NO_2) group in 5-NPPP was evaluated further on chances of having a role in enhancing the activity when combined with antibiotics. When the ALogP98 was evaluated against the PSA, most of the isosteres lay within the effective adsorption area of the eclipse (**Figure 3**).

Identification of *S. aureus* Clinical Strain Overexpressing NorA

Clinical strains of *S. aureus* were screened for resistance/sensitivity toward the broad spectrum of antibacterial agents that belongs to quinolones, fluoroquinolones, macrolide, penicillin, and cephalosporins. Among the clinical isolates, *Sa*-P1920, *Sa*-P2003, and *Sa*-EYE33 exhibited a multidrug resistance (MDR) phenotype. Also, a key observation was that the strain *Sa*-P2003 exhibited resistance to fluoroquinolones such as CIP and NOR (**Figure S1**). An earlier report suggests the involvement of the NorA efflux pump expelling fluoroquinolones and favoring the pathogens to acquire intrinsic resistance. So, we intend to explore the interrelationship of the NorA efflux pump expression by the MDR clinical isolates. The data were quite significant to show that the clinical isolate *Sa*-P2003 was observed to overexpress *norA*, as the cycle threshold (CT) value was several folds lesser in comparison with the other strains (**Figure S2**). The data were also in concordance with the EtBr efflux activity (data not shown).

Combinatorial Action of 5-NPPP With CIP

The potentiation activity of 5-NPPP with CIP was assessed using a checkerboard assay. The MIC of CIP against the strains SA-1199B and *Sa*-P2003 was evaluated to be 8 μg/ml. In the combination with 5-NPPP, the concentration of CIP against these two strains (**Figures 4B, D**) was drastically reduced to 0.5 μg/ml, having 16-fold reduction in MIC, thus proving its potentiating efficacy. In addition, the combinatorial action of

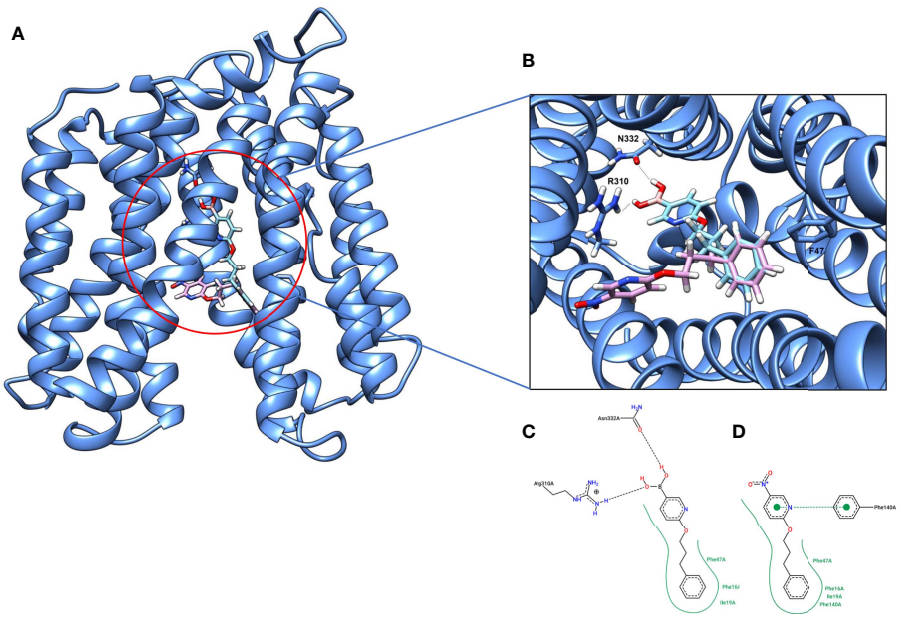

FIGURE 2 | **(A)** Hypothetical binding mode of 5-NPPP at the hydrophobic cleft of the NorA efflux pump (blue). The ligand is represented in a multicolor stick model. **(B)** The binding interactions of 6-(3-phenylpropoxy) pyridine-3-boronic acid and 5-NPP with the binding site amino acids. **(C)** 2D-interaction map of 6-(3-phenylpropoxy) pyridine-3-boronic acid with the NorA efflux pump. **(D)** 2D interaction map of 5-NPPP with the Nor A efflux pump in hydrophobic cleft with Phe47, Phe16, Phe140, and Ile19 enables a stronger hydrophobic interaction due to the closer proximity of the ligand with these residues as well as possessing π–π interactions.

5-NPPP and CIP was analyzed further by fitting into the ZIP model (**Figure 4A**). The ZIP model overcomes the drawbacks of other drug interaction models wherein the combined response does not affect the individual potency of the drugs. From the response plot, it can be observed that CIP showed a strong additive effect (score of 3.49) with 5-NPPP for *Sa*-P2003 (**Figure 4A**), whereas a strong synergism score of 12.31 was achieved for SA-1199B (**Figure 4C**). The scores are based on the cumulative evaluation of all the concentrations considered. A closer look reveals a 16-fold reduction in the ciprofloxacin concentration against both the strains. Thus, 5-NPPP significantly increases the bactericidal activity of CIP than the effect of either drug against *Sa*-P2003.

Evaluation of the 5-NPPP on EtBr Efflux Action

The clinical isolates *Sa*-P2003 and SA-1199B as independent trials were loaded with the known substrate (EtBr) of the NorA efflux pump either with or without 5-NPPP. The samples were placed in a fluorometer cuvette containing a fresh nutrient medium, and the assay was carried out for 30 min. There was a time-dependent decrease in the fluorescence that was observed due to the action NorA-mediated efflux of EtBr as maximal extrusion was observed in the control (untreated). On contrary, the cells treated with 5-NPPP showed prolonged retention of fluorescence, and the data were equivalent to the known EPI verapamil. In both the strains, ~76% reduction in the EtBr efflux was achieved by 5-NPPP treatment (**Figure 5**). A similar and comparable EtBr efflux reduction was achieved for the positive control, verapamil. The observed data suggest that, in the absence of 5-NPPP, the EtBr readily effluxes out of the cells *Sa*-P2003 and SA-1199B due to the action of the NorA as it is not favored to intercalate onto the DNA.

Evaluation of Cytotoxicity

The effect of 5-NPPP on host mammalian cells was analyzed using Hep-G2 cells. Three different concentrations, 1X MIC (400 μg mL^{-1}), 10X (4 μg mL^{-1}), and 100X (40 μg mL^{-1}), were tested, and the data revealed that, even at high concentration, 5-NPPP was nontoxic to Hep-G2 (**Figure 6**). Hence, 5-NPPP provides a possibility for the development of the nontoxic active molecule that could increase the antibacterial effect of fluoroquinolones against *S. aureus*.

DISCUSSION

The efficacy of boronic acid and its derivatives as effector molecules for the development of therapeutic agents has been well established (Albers et al., 2011; Maynard et al., 2014; Hecker et al., 2020). As a part of therapeutic potential, the antibacterial effect of boronic acid was known to suppress the production of virulence determinants and antibiotic-degrading enzymes to enhance the activity of antibiotics (Trippier and McGuigan, 2010). Similarly, a wide range of boronic acid derivatives has been explored for their therapeutic potential as β-lactamase

TABLE 2 | ADMET prediction of the screened bio isosteric molecules.

S.No.:	Compound	AlogP98	Polar Surface Area (PSA)	Hepatotoxic	CYPD26	Aqueous Solubility	BBB Penetration	Absorption
1	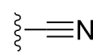	2.873	79.12	F	F	3	2	0
2	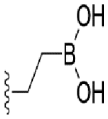	3.321	41.00	F	F	3	1	0
3	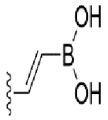	3.768	20.19	T	T	2	1	0
4	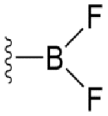	2.928	70.75	T	F	3	2	0
5	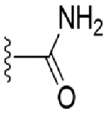	4.227	20.19	F	T	2	0	0
6	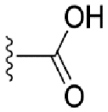	2.958	41.00	F	F	3	1	0
7		3.546	29.12	F	T	3	1	0
8		4.049	20.19	F	F	2	0	0
9	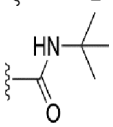	4.311	20.19	T	T	2	0	0
10		3.457	63.01	T	F	2	2	0
11		4.141	20.19	T	T	2	0	0
12	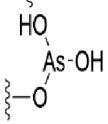	4.194	61.88	F	F	3	1	0
13		3.41	43.27	F	T	3	1	0
14	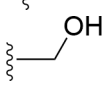	2.465	76.90	F	F	3	3	0
15	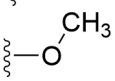	2.268	81.33	F	F	3	3	0
16	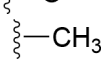	2.619	69.81	F	F	3	2	0
17		2.688	46.73	F	F	3	2	0
18	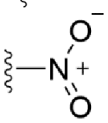	4.593	41.0	F	F	2	1	0
19		3.418	46.42	F	F	3	1	0
20	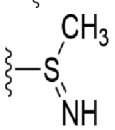	2.895	75.60	T	F	3	2	0

(Continued)

TABLE 2 | Continued

S.No.:	Compound	AlogP98	Polar Surface Area (PSA)	Hepatotoxic	CYPD26	Aqueous Solubility	BBB Penetration	Absorption
21	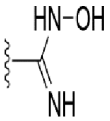	4.505	20.19	F	T	2	0	0
22	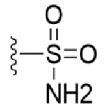	3.102	58.36	F	F	3	2	0
23	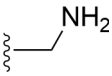	3.976	61.82	F	F	3	1	0
24	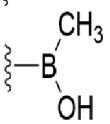	3.38	54.51	F	F	3	1	0
25	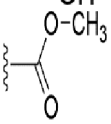	4.358	20.25	F	F	2	0	0
26	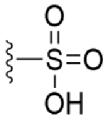	4.576	63.07	F	F	2	1	0
27		4.576	63.07	F	F	2	1	0
28	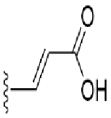	4.682	20.25	F	F	2	0	0
29	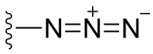	4.505	20.19	F	T	2	0	0
30	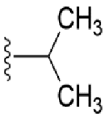	5.953	41.0	F	F	2	0	0
31	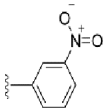	4.233	67.60	T	F	2	1	0
32	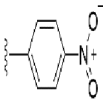	3.304	78.86	F	F	3	2	0
33	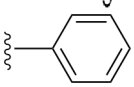	2.656	67.60	T	F	3	2	0
34	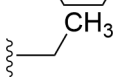	4.835	20.19	F	F	2	0	0
35	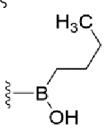	3.846	94.19	T	F	2	3	0

(Continued)

TABLE 2 | Continued

S.No.:	Compound	AlogP98	Polar Surface Area (PSA)	Hepatotoxic	CYPD26	Aqueous Solubility	BBB Penetration	Absorption
36	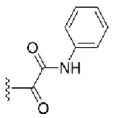	2.474	67.60	T	F	3	2	0
37	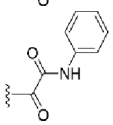	2.771	50.30	T	F	3	2	0
38	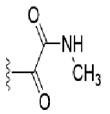	2.565	64.03	T	F	3	2	0
39	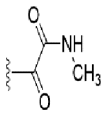	3.192	58.30	T	F	3	2	0
40	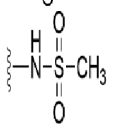	3.563	20.19	F	T	3	1	0
41	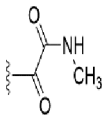	2.816	46.73	T	F	3	2	0
42	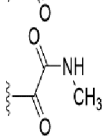	3.702	50.30	T	F	2	1	0

AlogP98 (≤ 2.0 or ≥ 7.0)—very poor absorption; PSA (≥ 150)—very low absorption; hepatotoxicity (T—True, F—False); CYPD26 (T—inhibitor, F—non-inhibitor); aqueous solubility (0—low; 1—very low, but possible; 2—low solubility; 3—good solubility; 4—optimal soluble; 5—too soluble); BBB penetration (0—very high penetration; 1—high penetration; 2—medium penetration; 3—low penetration; 4—undefined); absorption (0—good; 1—high; 2—medium; 3—low; 4—undefined).

inhibitors against class A and class C β-lactamases (Crompton et al., 1988; Tondi et al., 2010; Winkler et al., 2013; Cendron et al., 2019). Boronic acid transition state analogue inhibitors have been effective in subduing the β-lactamase-based resistance in *P. aeruginosa* (Eidam et al., 2012). Vabomere®, a drug composed of boronic acid and the β-lactam meropenem, has been marketed to treat urinary tract infections caused by (MDR) *Pseudomonas* and carbapenem-resistant *Enterobacteriaceae* (Griffith et al., 2019). Pentapeptide boronic acid inhibitors were effective against the $MycP_1$ protease of the Esx secretion system, one of the major virulence determinants of *Mycobacterium tuberculosis* (Frasinyuk et al., 2014; Cao et al., 2015; Bosserman and Champion, 2017). Recently, several pyridine-3-boronic acids were screened against NorA overproducing mutant *S. aureus* strain SA-1199B, and the pyridine-3- and benzene boronic acids were reported to be the most effective against NorA. The data also suggest that 6-benzyloxypyridine-3-boronic acid and 4-benzyloxybenzene boronic acid enhanced the antibacterial activity of CIP with minimum modulatory concentration (MMC) of 1.0 and 0.5 μg/ml, respectively (Fontaine et al., 2014). Further chemical pharmacomodulation revealed that 6-benzyloxypyridine-3-boronic acid could increase CIP activity by fourfold at 16 μg/ml against the NorA overexpressing strain, SA-1199B (Fontaine et al., 2015). However, some groups of boronic acids including the heterocyclic, cyclopropyl, and vinyl boronic acids have been reported to be unstable undergoing decomposition upon exposure to air through the process of oxidation, polymerization, and protodeboronation (Knapp et al., 2009). Based on these evidences, 6-benzyloxypyridine-3-boronic acid was chosen as the pharmaco-template for our study. In the present study, we intended to replace the boronic acid functional group from the template molecule using the bioisosteric approach to enhance the CIP potentiating activity from fourfold to several-fold. In this context, we could build about 42 replacement molecules through the Swiss Bioisostere tool. The 42 compounds that were generated were analyzed for the potential to interact with the NorA efflux pump by docking studies and their property for drug-likeness. The results indicate that many isosteres of the parent compound do interact with the target, and the ligands do possess significant solubility and adsorption potential. Further evaluation of their potential to get absorbed into the biological system revealed that about 39 compounds could be well absorbed into the human gut, and two molecules were known to cross the blood–brain barrier. For our current study, we have taken forwarded 5-NPPP having the nitro group in the place of the boron group by considering two aspects—

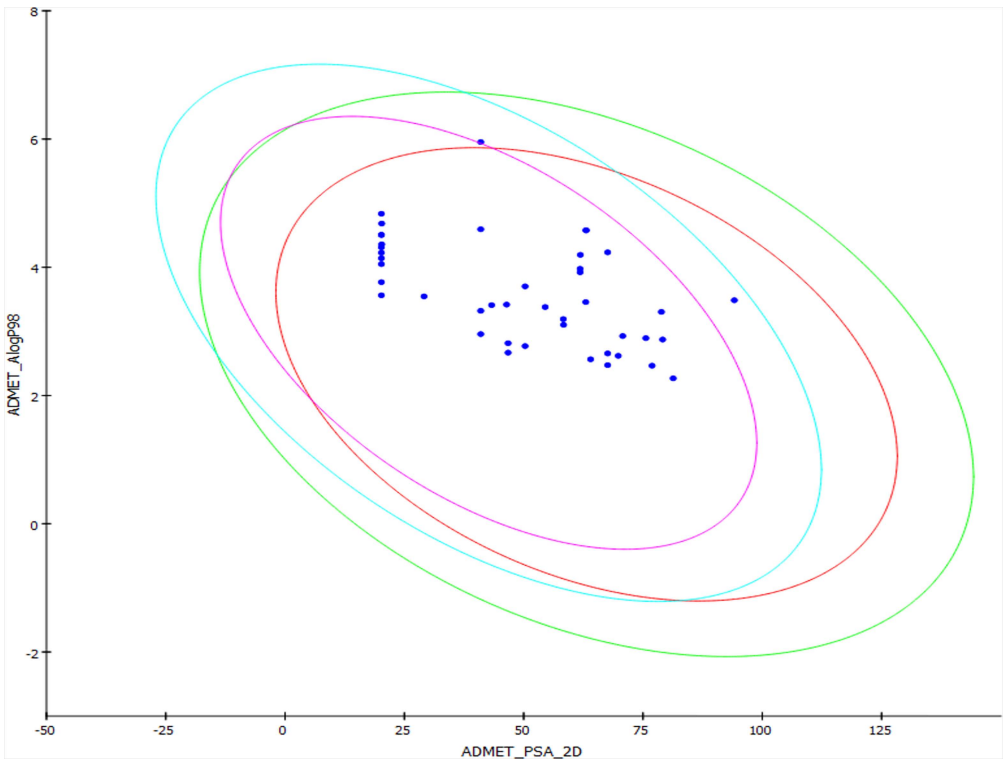

FIGURE 3 | ADME/T evaluation plot of PSA *vs* AlogP for 38 lead molecules; 99% and 95% confidence limits correspond to intestinal absorption and blood–brain barrier models.

ease of synthesis and biological significance. In the synthesis perspective, nitro groups can be introduced easily *via* any one of the following methods: (i) C-H nitration (Song et al., 2019), (ii) nitration in ionic liquid (Moosavi-Zare et al., 2016), (iii) copper-catalyzed mild nitration (Hernando et al., 2014), (iv) using a mild tert-butyl nitrite as the nitro source (Li et al., 2019), and (v) oxidation of aromatic amines (Ravi et al., 2019). Additionally, as these nitration processes are tolerant with various functional groups, the nitro group can be introduced to any biologically interesting core molecules without any change in the core structure (Kilpatrick et al., 2013).

The *in silico* ADMET studies revealed that 5-NPPP exhibited an AlogP98 score of 3.418 and PSA of 46.42 was chosen. Earlier studies predicted that the designing of NorA specific drugs targeting the amino acids Trp or Met or Phe has been suggested to modulate protein function effectively (Ma and Nussinov, 2007). Similarly, in our study, 5-NPPP interacts with the NorA protein in the phenylalanine group. Moreover, the interaction also occurs in the π–π interaction pattern, suggesting the exertion of van der Waal's forces to act upon the complex formed between the ligand and the target (**Figure 2**). A previous study has demonstrated that having various kinds of intermolecular interactions such as van der Waal's, alkyl-, π-sulfur, π–π, and π-alkyl is found to be responsible for the stability of the NorA complex with the ligands (Figueredo et al., 2020). The nitro group allows electron donation property, allowing further modulation of intracellular oxidative stress (Benites et al., 2010). Similarly, from the class of the indole group, the compound 5-nitro-2 phenylindole (INF55) was able to potentiate the action of CIP (1.5 μg/mL) with a fourfold increase against *S. aureus* (Markham et al., 1999). Modifying the structures at positions of C2, C3, and C5 in the primary discovered compounds has always preserved an electron-withdrawing group such as nitro in 1, 3, 4 or cyano group in 2 (Ambrus et al., 2008; Samosorn et al., 2009). It is interesting to note that indole-carrying halogen atoms in the C5 position and nitrone moiety in C3 are found to possess better EPI activity (Hequet et al., 2014). Nitro groups are known to resemble pro-drug, and reduction of nitro groups by enzymatic process leads to the formation of reactive species and exhibits therapeutic effects against bacterial pathogens (Wardman, 2001). A study has shown the reduction in the therapeutic potential of flutamide in the treatment of prostate cancer when the inherent nitro moiety of the drug was replaced with cyano (Coe et al., 2007). Similarly, when the nitro moiety was replaced with acetyl, benzoyl, methyl sulfone, or amide in the FDA-approved anthelmintic agent, niclosamide, the biological activity was significantly modified (Mook et al., 2015). Hence, the presence of the nitro group in the identified lead molecule, 5-NPPP, could potentially serve in resensitizing multidrug resistant *S. aureus* strains that overexpress the efflux pump NorA.

In this "post-antibiotic" era, several pathogens have developed multidrug resistance to most of the conventional

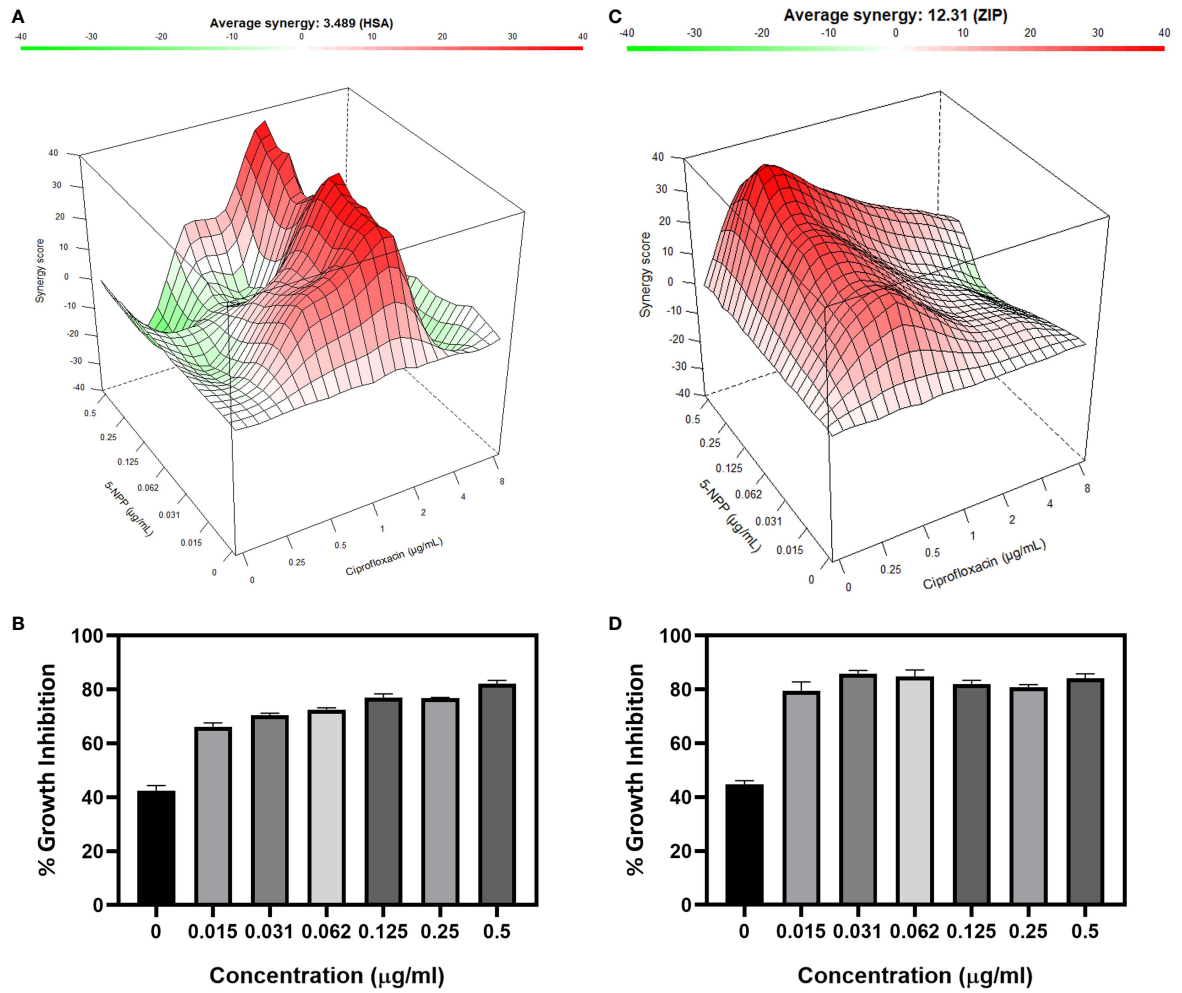

FIGURE 4 | Effect of 5-NPPP in enhancing the bactericidal potential of ciprofloxacin. **(A)** Synergy plot of *Sa*-P2003 at varying concentrations of ciprofloxacin and 5-NPPP. The synergy score of 3.489 (Highest Single Agent model) shows additive. **(B)** For *Sa*-P2003, at the constant concentration of ciprofloxacin (0.5 µg mL^{-1}), the concentration-dependent growth inhibitory activity of 5-NPPP is shown. **(C)** Synergy plot of SA-1199B at varying concentrations of ciprofloxacin and 5-NPPP. The zero-interaction potency model was used to fit the synergy data having the synergy score of 12.31, which shows synergism. **(D)** For SA-1199B, at the constant concentration of ciprofloxacin (0.5 µg mL^{-1}), the potentiation activity of 5-NPPP was established at the minimum concentration of 0.015 µg mL^{-1} (5-NPPP).

antibacterial and antifungals, which leads to the failure of treatment. Bacterial cells express antibiotic resistance through various mechanisms, and one such mechanism is through effusing the antibacterial agents across the outer membrane by efflux pumps. About 10 plasmids or chromosome encoded multidrug efflux pumps have been defined in *S. aureus*, some of which can expel structurally diverse antibacterial agents (Piddock, 2006; Costa et al., 2013). Thus, the development of EPI, which blocks the efflux pump action, is essential to overcome the antibiotic resistance mechanisms. The major efflux pumps of *S. aureus* including NorA, NorB, NorC, SdrM, MdeA, LmrS, QacA, QacB, Tet38, and TetA (K) belong to the MFS (Yoshida et al., 1990; Huang et al., 2004; Truong-Bolduc et al., 2005; Truong-Bolduc et al., 2006; Yamada et al., 2006; Lekshmi et al., 2018). Among these multidrug efflux pumps, *norA* confers *S. aureus* the ability to resist the antibacterial effect of hydrophilic quinolones such as CIP, NOR, ofloxacin, and enoxacin, and less or complete susceptibility to hydrophobic quinolones (Yoshida, 1992). When a strain overexpresses *nor*A, a high level of NorA protein accumulates in the cytoplasmic membrane. Thereby, *S. aureus* strains resist fluoroquinolones (Kaatz and Seo, 1995). In this regard, the effluxing activity of the overexpressing strains was significantly reduced in the presence of 5-NPPP (76% inhibition), which is comparable to the positive control, Verapamil (Aeschlimann et al., 1999). This proves that our modification has enhanced the efflux pump inhibitory effect. Moreover, fluoroquinolones including CIP and NOR are suitable substrates for NorA protein (Singh et al., 2017). Alteration in the expression of *norA* connects intrinsic CIP resistance and evolvability. Suppressing NorA in the clinical strains had resulted in the borderline loss of resistance in *S. aureus* 16 (Papkou et al., 2020). Many chemically diverse NorA inhibitors

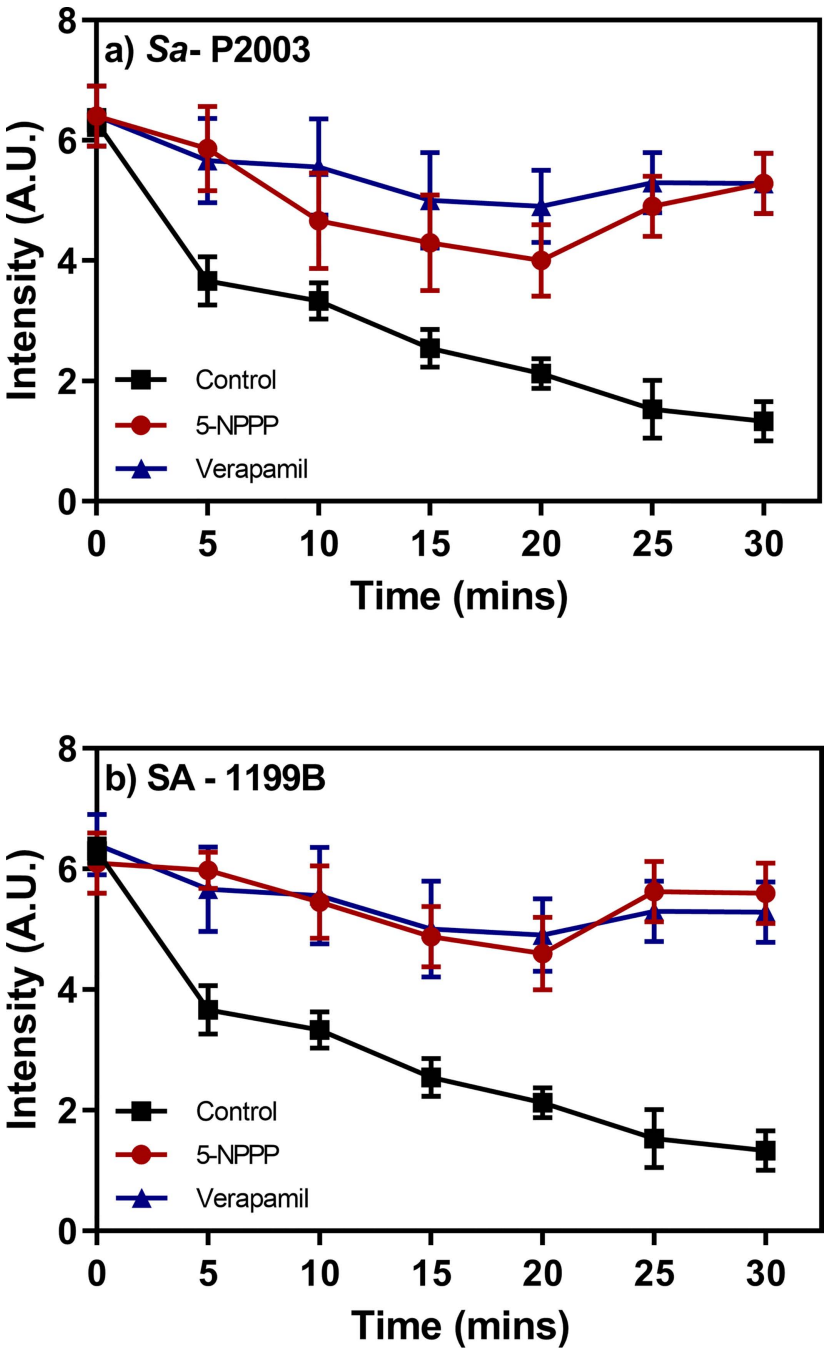

FIGURE 5 | Evaluation of the effect of the identified NorA efflux pump efflux and the accumulation of ethidium bromide in **(A)** *Sa*-P2003 and **(B)** SA-1199B. Verapamil is included as positive control, and the efflux activity without the addition of any drug is considered as a negative control.

that synergistically increase the bactericidal efficacy of CIP in NorA overexpressing *S. aureus* strain had been reported. In this regard, 5-NPPP was shown to reduce the concentration of CIP 16-fold. The MIC of 0.5 μg/ml was achieved by the presence of 5-NPPP, thus proving the enhanced potentiating activity of 5-NPPP. Furthermore, our study has demonstrated that, at very minimal concentration without toxicity to mammalian cells, 5-NPPP in combination with CIP increased the susceptibility of MDR *Sa*-P2003 and SA-1199B through inhibition of the efflux pump NorA.

Thus, the current work identifies a novel derivative of boronic species 5-NPPP as the effective EPI against the NorA overexpressing strains. The preliminary studies on 5-NPPP effectively prove the significant reduction in the EtBr efflux, the potentiating activity of the CIP to 16-fold reduction, and minimal

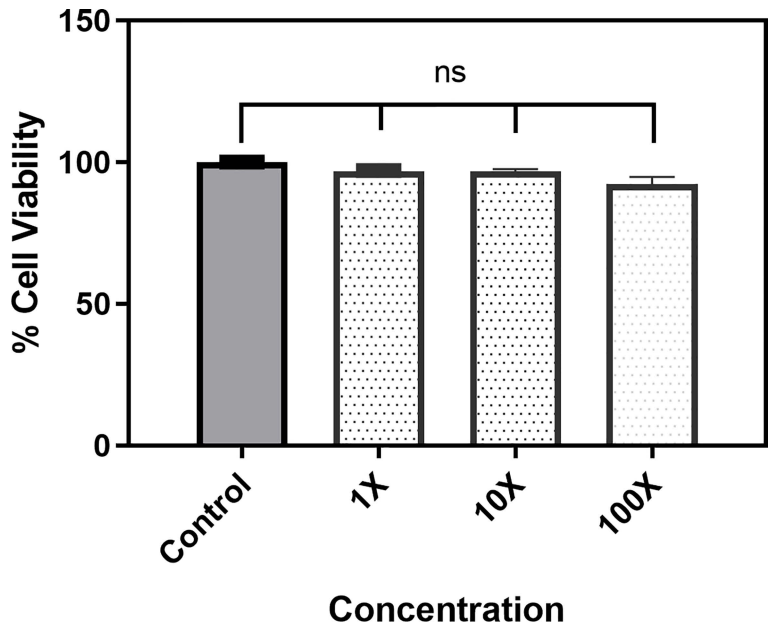

FIGURE 6 | Cytotoxicity assay. The bar graph depicts the viability of the Hep-G2 in the presence of 1X, 10X, and 100X of the 5-NPPP. ns, non-significant.

mammalian cell toxicity. This paves the path to explore this compound further in terms of the pharmacokinetic and pharmacodynamic studies. Future studies are under steady progress to exploit 5-NPPP in *in vivo* infectious models.

DATA AVAILABILITY STATEMENT

The original contributions presented in the study are included in the article/**Supplementary Material**. Further inquiries can be directed to the corresponding author.

AUTHOR CONTRIBUTIONS

Study conception design and project administration: APS. Computational data analysis and interpretation of results: GT, AS, and KS. 5-NPPP synthesis and characterization: GT and PV. In vitro data acquiring: GT. In vitro data analysis and interpretation of results: GT and APS. Original draft manuscript preparation, writing, reviewing, and editing: GT, HB, SV, and APS. All authors have read and agreed to publish this version of the manuscript.

ACKNOWLEDGMENTS

TG wishes to express his gratitude to SASTRA Deemed to be University for providing him an opportunity to carry out the present work as a part of his Ph.D. dissertation work. GT also thanks his colleagues, Sahana Vasudevan (SV) and Hema Bhagavathi (HB), for their continuous moral support throughout the work. TG, KS, AS, VP, and SAP acknowledge SASTRA Deemed to be University, Thanjavur, for extending support to use the Schrödinger software suite for carrying out *in silico* studies and Professor Sumana (Department of Microbiology, JSS Medical College and JSS University, India) for the clinical *S. aureus* strains. Also, it is sincerely acknowledged that we received the following strains through BEI Resources, NIAID, NIH: *Staphylococcus aureus*, Strain SA-1199B, NR-51189, SA-1199, and NR-51188.

SUPPLEMENTARY MATERIAL

The Supplementary Material for this article can be found online at: https://www.frontiersin.org/articles/10.3389/fcimb.2021.700198/full#supplementary-material

REFERENCES

Aeschlimann, J. R., Dresser, L. D., Kaatz, G. W., and Rybak, M. J. (1999). Effects of NorA Inhibitors on *In Vitro* Antibacterial Activities and Post Antibiotic Effects of Levofloxacin, Ciprofloxacin, and Norfloxacin in Genetically Related Strains of Staphylococcus Aureus. *Antimicrob. Agents Chemother.* 43 (2), 335–340. doi: 10.1128/aac.43.2.335

Albers, H. M. H. G., Hendrickx, L. J. D., Van Tol, R. J. P., Hausmann, J., Perrakis, A., and Ovaa, H. (2011). Structure-Based Design of Novel Boronic Acid-Based Inhibitors of Autotaxin. *J. Med. Chem.* 54 (13), 4619–4626. doi: 10.1021/jm200310q

Ambrus, J. I., Kelso, M. J., Bremner, J. B., Ball, A. R., Casadei, G., and Lewis, K. (2008). Structure-Activity Relationships of 2-Aryl-1H-Indole Inhibitors of the NorA Efflux Pump in Staphylococcus Aureus. *Bioorg. Med. Chem. Lett.* 18 (15), 4294–4297. doi: 10.1016/j.bmcl.2008.06.093

Astolfi, A., Felicetti, T., Iraci, N., Manfroni, G., Massari, S., Pietrella, D., et al. (2017). Pharmacophore-Based Repositioning of Approved Drugs as Novel Staphylococcus Aureus NorA Efflux Pump Inhibitors. *J. Med. Chem.* 60 (4), 1598–1604. doi: 10.1021/acs.jmedchem.6b01439

Balasubramanian, S., Chandy, S., Peter, R., Nachiyar, G. S., Sudhakar, A., Sumanth, A., et al. (2020). Utility of a Multiplex Real-Time Polymerase Chain Reaction for Combined Detection and Serotyping of Dengue Virus in Pediatric Patients Hospitalised With Severe Dengue: A Report From Chennai. Indian. *J. Med. Microbiol.* 38, 3&4. doi: 10.4103/ijmm.ijmm_20_249

Benites, J., Valderrama, J. A., Bettega, K., Pedrosa, R. C., Calderon, P. B., and Verrax, J. (2010). Biological Evaluation of Donor-Acceptor Aminonaphthoquinones as Antitumor Agents. *Eur. J. Med. Chem.* 45 (12), 6052–6057. doi: 10.1016/j.ejmech.2010.10.006

Billingsley, K. L., and Buchwald, S. L. (2008). An Improved System for the Palladium-Catalyzed Borylation of Aryl Halides With Pinacol Borane. *J. Org. Chem.* 73 (14), 5589–5591. doi: 10.1021/jo800727s

Blair, J. M. A., Webber, M. A., Baylay, A. J., Ogbolu, D. O., and Piddock, L. J. V. (2015). Molecular Mechanisms of Antibiotic Resistance. *Nat. Rev. Microbiol.* 13 (1), 42–51. doi: 10.1038/nrmicro3380

Bosserman, R. E., and Champion, P. A. (2017). Esx Systems and the Mycobacterial Cell Envelope: What's the Connection? *J. Bacteriol.* 199, 17. doi: 10.1128/jb.00131-17

Brenwald, N. P., Gill, M. J., and Wise, R. (1998). Prevalence of a Putative Efflux Mechanism Among Fluoroquinolone-Resistant Clinical Isolates of Streptococcus Pneumoniae. *Antimicrob. Agents Chemother.* 42 (8), 2032–2035. doi: 10.1128/aac.42.8.2032

Cao, G., Howard, S. T., Zhang, P., Wang, X., Chen, X. L., Samten, B., et al. (2015). EspR, a Regulator of the ESX-1 Secretion System in Mycobacterium Tuberculosis, Is Directly Regulated by the Two-Component Systems mprAB and phoPR. *Microbiology* 161 (3), 477–489. doi: 10.1099/mic.0.000023

Cendron, L., Quotadamo, A., Maso, L., Bellio, P., Montanari, M., Celenza, G., et al. (2019). X-Ray Crystallography Deciphers the Activity of Broad-Spectrum Boronic Acid β-Lactamase Inhibitors. *ACS Med. Chem. Lett.* 10 (4), 650–655. doi: 10.1021/acsmedchemlett.8b00607

Clary, J. W., Rettenmaier, T. J., Snelling, R., Bryks, W., Banwell, J., Wipke, W. T., et al. (2011). Hydride as a Leaving Group in the Reaction of Pinacolborane With Halides Under Ambient Grignard and Barbier Conditions. One-Pot Synthesis of Alkyl, Aryl, Heteroaryl, Vinyl, and Allyl Pinacolboronic Esters. *J. Org. Chem.* 76 (23), 9602–9610. doi: 10.1021/jo201093u

Cloete, R, Kapp, E., Joubert, J., Christoffels, I., Malan, S. F., et al. (2018). Molecular Odelling And Simulation Studies Of The Mycobacterium Tuberculosis Multidrug Efflux Pump Protein Rv1258c. *PlosOne* 13 (11), e0207605. doi: 10.1371/journal.pone.0207605

Coe, K. J., Jia, Y., Ho, H. K., Rademacher, P., Bammler, T. K., Beyer, R. P., et al. (2007). Comparison of the Cytotoxicity of the Nitroaromatic Drug Flutamide to Its Cyano Analogue in the Hepatocyte Cell Line TAMH: Evidence for Complex I Inhibition and Mitochondrial Dysfunction Using Toxicogenomic Screening. *Chem. Res. Toxicol.* 20 (9), 1277–1290. doi: 10.1021/tx7001349

Costa, S. S., Viveiros, M., Amaral, L., and Couto, I. (2013). Multidrug Efflux Pumps in Staphylococcus Aureus: An Update. *Open Microbiol. J.* 7, 59–71. doi: 10.2174/1874285801307010059

Crompton, I. E., Cuthbert, B. K., Lowe, G., and Waley, S. G. (1988). Beta-Lactamase Inhibitors. The Inhibition of Serine Beta-Lactamases by Specific Boronic Acids. *Biochem. J.* 251 (2), 453–459. doi: 10.1042/bj2510453

Das, S., Alexeev, V. L., Sharma, S. C., Geib, S. J., and Asher, S. A. (2003). Synthesis and Crystal Structure of 4-Amino-3-Fluorophenylboronic Acid. *Tetrahedron Lett.* 44 (42), 7719 – 7722. doi: 10.1016/j.tetlet.2003.08.094

Eidam, O., Romagnoli, C., Dalmasso, G., Barelier, S., Caselli, E., Bonnet, R., et al. (2012). Fragment-Guided Design of Subnanomolar β-Lactamase Inhibitors Active *In Vivo*. *Proc. Natl. Acad. Sci.* 109 (43), 17448–17453. doi: 10.1073/pnas.1208337109

Felicetti, T., Cannalire, R., Burali, M. S., Massari, S., Manfroni, G., Barreca, M. L., et al. (2017). Searching for Novel Inhibitors of the S. Aureus NorA Efflux Pump: Synthesis and Biological Evaluation of the 3-Phenyl-1,4-Benzothiazine Analogues. *ChemMedChem* 12 (16), 1293–1302. doi: 10.1002/cmdc.201700286

Fernandes, P. (2006). Antibacterial Discovery and Development–the Failure of Success? *Nat. Biotechnol.* 24 (12), 1497–1503. doi: 10.1038/nbt1206-1497

Figueredo, F. G., Ramos, I. T. L., Paz, J. A., Silva, T. M. S., Câmara, C. A., de Morais Oliveira-Tintino, C. D., et al. (2020). Effect of Hydroxyamines Derived From Lapachol and Norlachol Against Staphylococcus Aureus Strains Carrying the NorA Efflux Pump. *Infect. Genet. Evol.* 84, 104370. doi: 10.1016/j.meegid.2020.104370

Fontaine, F., Héquet, A., Voisin-Chiret, A. S., Bouillon, A., Lesnard, A., Cresteil, T., et al. (2014). First Identification of Boronic Species as Novel Potential Inhibitors of the Staphylococcus Aureus NorA Efflux Pump. *J. Med. Chem.* 57 (6), 2536–2548. doi: 10.1021/jm401808n

Fontaine, F., Héquet, A., Voisin-Chiret, A. S., Bouillon, A., Lesnard, A., Cresteil, T., et al. (2015). Boronic Species as Promising Inhibitors of the Staphylococcus Aureus NorA Efflux Pump: Study of 6-Substituted Pyridine-3-Boronic Acid Derivatives. *Eur. J. Med. Chem.* 95, 185–198. doi: 10.1016/j.ejmech.2015.02.056

Frasinyuk, M. S., Kwiatkowski, S., Wagner, J. M., Evans, T. J., Reed, R. W., Korotkov, K. V., et al. (2014). Pentapeptide Boronic Acid Inhibitors of Mycobacterium Tuberculosis MycP1 Protease. *Bioorg. Med. Chem. Lett.* 24 (15), 3546–3548. doi: 10.1016/j.bmcl.2014.05.056

Friesner, R. A., Murphy, ,. R. B., Reapasky, M. P., Frye, L. L., Grrenwood, J. R., Halgren, T. A., et al. (2006). Extra Precision Glide: Docking and Scoring Incorporating a Model of Hydrophobic Enclosure for Protein–Ligand Complexes. *J. Med. Chem.* 49 (21), 6177–6196. doi: 10.1021/jm051256o

Griffith, D. C., Sabet, M., Tarazi, Z., Lomovskaya, O., and Dudley, M. N. (2019). Pharmacokinetics/Pharmacodynamics of Vaborbactam, a Novel Beta-Lactamase Inhibitor, in Combination With Meropenem. *Antimicrob. Agents Chemother.* 63 (1), e01659–e01618. doi: 10.1128/aac.01659-18

Hafner, A., Meisenbach, M., and Sedelmeier, J. (2016). Flow Chemistry on Multigram Scale: Continuous Synthesis of Boronic Acids Within 1 s. *Org. Lett.* 18 (15), 3630–3633. doi: 10.1021/acs.orglett.6b01681

Hartmann, M., Berditsch, M., Hawecker, J., Ardakani, M. F., Gerthsen, D., and Ulrich, A. S. (2010). Damage of the Bacterial Cell Envelope by Antimicrobial Peptides Gramicidin S and PGLa as Revealed by Transmission and Scanning Electron Microscopy. *Antimicrob. Agents Chemother.* 54 (8), 3132–3142. doi: 10.1128/aac.00124-10

Hecker, S. J., Reddy, K. R., Lomovskaya, O., Griffith, D. C., Rubio-Aparicio, D., Nelson, K., et al. (2020). Discovery of Cyclic Boronic Acid QPX7728, an Ultrabroad-Spectrum Inhibitor of Serine and Metallo-β-Lactamases. *J. Med. Chem.* 63 (14), 7491–7507. doi: 10.1021/acs.jmedchem.9b01976

Hequet, A., Burchak, O. N., Jeanty, M., Guinchard, X., Le Pihive, E., Maigre, L., et al. (2014). 1-(1H-Indol-3-Yl)Ethanamine Derivatives as Potent Staphylococcus Aureus NorA Efflux Pump Inhibitors. *ChemMedChem* 9 (7), 1534–1545. doi: 10.1002/cmdc.201400042

Hernando, E., Castillo, R. R., Rodríguez, N., Gomez Arrayas, R., and Carretero, J. C. (2014). Copper-Catalyzed Mild Nitration of Protected Anilines. *Chem. Eur. J.* 20 (43), 13854–13859. doi: 10.1002/chem.201404000

Huang, J., O'Toole, P. W., Shen, W., Amrine-Madsen, H., Jiang, X., Lobo, N., et al. (2004). Novel Chromosomally Encoded Multidrug Efflux Transporter MdeA in Staphylococcus Aureus. *Antimicrob. Agents Chemother.* 48 (3), 909–917. doi: 10.1128/aac.48.3.909-917.2004

Jiang, M., Yang, H., and Fu, H. (2016). Visible-Light Photoredox Borylation of Aryl Halides and Subsequent Aerobic Oxidative Hydroxylation. *Org. Lett.* 18 (20), 5248–5251. doi: 10.1021/acs.orglett.6b02553

Kaatz, G. W., and Seo, S. M. (1995). Inducible NorA-Mediated Multidrug Resistance in Staphylococcus Aureus. *Antimicrob. Agents Chemother.* 39 (12), 2650–2655. doi: 10.1128/aac.39.12.2650

Kakhki, S., Shahosseini, S., and Zarghi, A. (2014). Design, Synthesis and Cytotoxicity Evaluation of New 2-Aryl-5, 6-Dihydropyrrolo[2, 1-a]Isoquinoline Derivatives as Topoisomerase Inhibitors. *Iran. J. Pharm. Res.* 13, 71–77.

Kalia, N. P., Mahajan, P., Mehra, R., Nargotra, A., Sharma, J. P., Koul, S., et al. (2012). Capsaicin, a Novel Inhibitor of the NorA Efflux Pump, Reduces the Intracellular Invasion of Staphylococcus Aureus. *J. Antimicrob. Chemother.* 67 (10), 2401–2408. doi: 10.1093/jac/dks232

Kilpatrick, B., Heller, M., and Arns, S. (2013). Chemoselective Nitration of Aromatic Sulfonamides With Tert-Butyl Nitrite. *Chem. Commun.* 49 (5), 514–516. doi: 10.1039/C2CC37481A

Knapp, D. M., Gillis, E. P., and Burke, M. D. (2009). A General Solution for Unstable Boronic Acids: Slow-Release Cross-Coupling From Air-Stable MIDA Boronates. *J. Am. Chem. Soc* 131 (20), 6961–6963. doi: 10.1021/ja901416p

Lan, L., Cheng, A., Dunman, P. M., Missiakas, D., and He, C. (2010). Golden Pigment Production and Virulence Gene Expression are Affected by Metabolisms in Staphylococcus Aureus. *J. Bacteriol.* 192 (12), 3068–3077. doi: 10.1128/jb.00928-09.,3068–3077

Leermann, T., Leroux, F. R., and Colobert, F. (2011). Highly Efficient One-Pot Access to Functionalized Arylboronic Acids *via* Noncryogenic Bromine/Magnesium Exchanges. *Org. Lett.* 13 (17), 4479–4481. doi: 10.1021/ol2016252

Lekshmi, M., Ammini, P., Adjei, J., Sanford, L. M., Shrestha, U., Kumar, S., et al. (2018). Modulation of Antimicrobial Efflux Pumps of the Major Facilitator Superfamily in Staphylococcus Aureus. *AIMS Microbiol.* 4 (1), 1–18. doi: 10.3934/microbiol.2018.1.1

Li, J., Qin, Z., Zhang, C., Zhang, Y., and Wen, C. (2019). Copper-Catalyzed C-H Bis-Nitration of 1-Naphthylamide Derivatives With Tert-Butyl Nitrite as Nitro Source. *Chem. Select* 4 (26), 7660–7664. doi: 10.1002/slct.201901177

Lipinski, C. A., Lombardo, F., Dominy, B. W., and Feeney, P. J. (2001). Experimental and Computational Approaches to Estimate Solubility and Permeability in Drug Discovery and Development Settings. *Adv. Drug Deliv. Rev.* 46 (1-3), 3–26. doi: 10.1016/s0169-409x(00)00129-0

Ma, B., and Nussinov, R. (2007). Trp/Met/Phe Hot Spots in Protein-Protein Interactions: Potential Targets in Drug Design. *Curr. Top. Med. Chem.* 7 (10), 999–1005. doi: 10.2174/156802607780906717

Markham, P. N., Westhaus, E., Klyachko, K., Johnson, M. E., and Neyfakh, A. A. (1999). Multiple Novel Inhibitors of the NorA Multidrug Transporter of Staphylococcus Aureus. *Antimicrob. Agents Chemother.* 43 (10), 2404–2408. doi: 10.1128/AAC.43.10.2404

Marquez, B. (2005). Bacterial Efflux Systems and Efflux Pumps Inhibitors. *Biochimie* 87 (12), 1137–1147. doi: 10.1016/j.biochi.2005.04.012

Maynard, A., Crosby, R. M., Ellis, B., Hamatake, R., Hong, Z., Johns, B. A., et al. (2014). Discovery of a Potent Boronic Acid-Derived Inhibitor of the HCV RNA-Dependent RNA Polymerase. *J. Med. Chem.* 57 (5), 1902–1913. doi: 10.1021/jm400317w,1902–1913

Mook, R. A. J., Wang, J., Ren, X.-R., Chen, M., Spasojevic, I., Barak, L. S., et al. (2015). Structure-Activity Studies of Wnt/β-Catenin Inhibition in the Niclosamide Chemotype: Identification of Derivatives With Improved Drug Exposure. *Bioorg. Med. Chem.* 23 (17), 5829–5838. doi: 10.1016/j.bmc.2015.07.001

Moosavi-Zare, A. R., Zolfigol, M. A., Zarei, M., Noroozizadeh, E., and Beyzavi, M. H. (2016). Nitration of Arenes by 1-Sulfopyridinium Nitrate as an Ionic Liquid and Reagent by *in Situ* Generation of NO_2. *RSC Adv.* 6, 89572–89577. doi: 10.1039/C6RA15922B

Neyfakh, A. A. (2002). Mystery of Multidrug Transporters: The Answer can be Simple. *Mol. Microbiol.* 44 (5), 1123–1130. doi: 10.1046/j.1365-2958.2002.02965.x

Papkou, A., Hedge, J., Kapel, N., Young, B., and MacLean, R. C. (2020). Efflux Pump Activity Potentiates the Evolution of Antibiotic Resistance Across S. Aureus Isolates. *Nat. Commun.* 11 (1), 3970. doi: 10.1038/s41467-020-17735-y

Patani, G. A., and LaVoie, E. J. (1996). Bioisosterism: A Rational Approach in Drug Design. *Chem. Rev.* 96 (8), 3147–3176. doi: 10.1021/cr950066q

Piddock, L. J. V. (2006). Clinically Relevant Chromosomally Encoded Multidrug Resistance Efflux Pumps in Bacteria. *Clin. Microbiol. Rev.* 19 (2), 382–402. doi: 10.1128/CMR.19.2.382-402.2006

Poole, K., and Lomovskaya, O. (2006). Can Efflux Inhibitors Really Counter Resistance? *Drug Discov. Today Ther. Strateg.* 3 (2), 145–152. doi: 10.1016/j.ddstr.2006.05.005

Ravi, K., Bankar, B. D., Jindani, S., and Biradar, A. V. (2019). Surfactant-Assisted Selective Oxidation of Aromatic Amines to Nitro Compounds by in Situ-Formed Performic Acid. *ACS Omega* 4 (5), 9453–9457. doi: 10.1021/acsomega.9b00543

Rodriguez-Tudela, J. L., Barchiesi, F., Bille, J., Chryssanthou, E., Cuenca-Estrella, M., and Denning, D. (2003). Method for the Determination of Minimum Inhibitory Concentration (MIC) by Broth Dilution of Fermentative Yeasts. *Clinical Microbiology and Infection* 9 (8), i–viii.

Sabatini, S., Gosetto, F., Iraci, N., Barreca, M. L., Massari, S., Sancineto, L., et al. (2013). Re-Evolution of the 2-Phenylquinolines: Ligand-Based Design, Synthesis, and Biological Evaluation of a Potent New Class of Staphylococcus Aureus NorA Efflux Pump Inhibitors to Combat Antimicrobial Resistance. *J. Med. Chem.* 56 (12), 4975–4989. doi: 10.1021/jm400262a

Sabatini, S., Gosetto, F., Manfroni, G., Tabarrini, O., Kaatz, G. W., Patel, D., et al. (2011). Evolution From a Natural Flavones Nucleus to Obtain 2-(4-Propoxyphenyl)quinoline Derivatives as Potent Inhibitors of the S. Aureus NorA Efflux Pump. *J. Med. Chem.* 54 (16), 5722–5736. doi: 10.1021/jm200370y

Sabatini, S., Gosetto, F., Serritella, S., Manfroni, G., Tabarrini, O., Iraci, N., et al. (2012). Pyrazolo[4,3-C][1,2]Benzothiazines 5,5-Dioxide: A Promising New Class of Staphylococcus Aureus NorA Efflux Pump Inhibitors. *J. Med. Chem.* 55 (7), 3568–3572. doi: 10.1021/jm201446h

Samosorn, S., Tanwirat, B., Muhamad, N., Casadei, G., Tomkiewicz, D., Lewis, K., et al. (2009). Antibacterial Activity of Berberine-NorA Pump Inhibitor Hybrids With a Methylene Ether Linking Group. *Bioorg. Med. Chem.* 17 (11), 3866–3872. doi: 10.1016/j.bmc.2009.04.028

Sangwan, P. L., Koul, J. L., Koul, S., Reddy, M. V., Thota, N., Khan, I. A., et al. (2008). Piperine Analogs as Potent Staphylococcus Aureus NorA Efflux Pump Inhibitors. *Bioorg. Med. Chem.* 16 (22), 9847–9857. doi: 10.1016/j.bmc.2008.09.042

Sastry, G. M., Adzhigirey, M., Day, T., Annabhimoju, R., and Sherman, W. (2013). Protein and Ligand Preparation: Parameters, Protocols, and Influence on Virtual Screening Enrichments. *J. Comput. Aided Mol. Des.* 27 (3), 221–234. doi: 10.1007/s10822-013-9644-8

Schillaci, D., Spanò, V., Parrino, B., Carbone, A., Montalbano, A., Barraja, P., et al. (2017). Pharmaceutical Approaches to Target Antibiotic Resistance Mechanisms. *J. Med. Chem.* 60 (20), 8268–8297. doi: 10.1021/acs.jmedchem.7b00215

Schmittgen, T. D., and Livak, K. J. (2008). Analyzing Real-Time PCR Data by the Comparative C(T) Method. *Nat. Protoc.* 3 (6), 1101–1108. doi: 10.1038/nprot.2008.73

Sharp, M. J., Cheng, W., and Snieckus, V. (1987). Synthetic Connections to the Aromatic Directed Metalation Reaction. Functionalized Aryl Boronic Acids by Ipso Borodesilylation. General Syntheses of Unsymmetrical Biphenyls and M-Terphenyls. *Tetrahedron Lett.* 28 (43), 5093–5096. doi: 10.1016/S0040-4039(00)95599-0

Sharp, M. J., and Snieckus, V. (1985). Synthetic Connections to the Aromatic Directed Metalation Reaction. Unsymmetrical Biaryls by Palladium-Catalyzed Cross Coupling of Directed Metalation-Derived Arylboronic Acids With Aryl Halides. *Tetrahedron Lett.* 26 (49), 5997–6000. doi: 10.1016/S0040-4039(00)95108-6

Shinzato, T., Sato, R., Suzuki, K., Tomioka, S., Sogawa, H., Shulga, S., et al. (2020). Proposal of Therapeutic Curcumin Derivatives for Alzheimer's Disease Based on Ab Initio Molecular Simulations. *Chem. Phys. Lett. Elsevier* 738, 136883. doi: 10.1016/j.cplett.2019.136883

Singh, S., Kalia, N. P., Joshi, P., Kumar, A., Sharma, P. R., Kumar, A., et al. (2017). Boeravinone B, A Novel Dual Inhibitor of NorA Bacterial Efflux Pump of Staphylococcus Aureus and Human P-Glycoprotein, Reduces the Biofilm Formation and Intracellular Invasion of Bacteria. *Front. Microbiol.* 8, 1868 (8). doi: 10.3389/fmicb.2017.01868

Song, L. R., Fan, Z., and Zhang, A. (2019). Recent Advances in Transition Metal-Catalyzed C (Sp 2)–H Nitration. *Org. Biomol. Chem.* 17 (6), 1351–1361. doi: 10.1039/C8OB02750A

Sun, J., Deng, Z., and Yan, A. (2014). Bacterial Multidrug Efflux Pumps: Mechanisms, Physiology, and Pharmacological Exploitations. *Biochem. Biophys. Res. Commun.* 453 (2), 254–267. doi: 10.1016/j.bbrc.2014.05.090

Tinoush, B., Shirdel, I., and Wink, M. (2020). Phytochemicals: Potential Lead Molecules for MDR Reversal. *Front. Pharmacol.* 11, 832. doi: 10.3389/fphar.2020.00832

Tomoari, K., Tadahiro, K., and Williams, D. (2014). *Chapter Thirteen - Antimicrobial Chemotherapy: Significance to Healthcare Biofilms in Infection Prevention and Control A Healthcare Handbook* (Academic Press), USA, 209–244.

Tondi, D., Calo, S., Shoichet, B. K., and Costi, M. P. (2010). Structural Study of Phenyl Boronic Acid Derivatives as AmpC Beta-Lactamase Inhibitors. *Bioorg. Med. Chem. Lett.* 20 (11), 3416–3419. doi: 10.1016/j.bmcl.2010.04.007

Trippier, P. C., and McGuigan, C. (2010). Boronic Acids in Medicinal Chemistry: Anticancer, Antibacterial and Antiviral Applications. *Medchemcomm* 1 (3), 183–198. doi: 10.1039/c0md00119h

Truong-Bolduc, Q. C., Dunman, P. M., Strahilevitz, J., Projan, S. J., and Hooper, D. C. (2005). Mgra Is a Multiple Regulator of Two New Efflux Pumps

in *Staphylococcus Aureus*. *J. Bacteriol.* 187 (7), 2395–2405. doi: 10.1128/JB.187.7.2395-2405.2005

Truong-Bolduc, Q. C., Strahilevitz, J., and Hooper, D. C. (2006). NorC, a New Efflux Pump Regulated by MgrA of Staphylococcus Aureus. *Antimicrob. Agents Chemother.* 50 (3), 1104–1107. doi: 10.1128/aac.50.3.1104-1107.2006

Tugal, D., Lynch, M., Hujer, A. M., Rudin, S., Perez, F., and Bonomo, R. A. (2015). Multi-Drug-Resistant Klebsiella Pneumoniae Pancreatitis: A New Challenge in a Serious Surgical Infection. *Surg. Infect.* 16 (2), 188–193. doi: 10.1089/sur.2012.175

Wardman, P. (2001). Electron Transfer and Oxidative Stress as Key Factors in the Design of Drugs Selectively Active in Hypoxia. *Curr. Med. Chem.* 8 (7), 739–761. doi: 10.2174/0929867013372959

Wikler, M. A. (2006). Methods For Dilution Antimicrobial Susceptibility Tests For Bacteria That Grow Aerobically: Approved Standard. CLSI (NCCLS). 26, M7-A7.

Winkler, M. L., Rodkey, E. A., Taracila, M. A., Drawz, S. M., Bethel, C. R., Papp-Wallace, K. M., et al. (2013). Design and Exploration of Novel Boronic Acid Inhibitors Reveals Important Interactions With a Clavulanic Acid-Resistant Sulfhydryl-Variable (SHV) β-Lactamase. *J. Med. Chem.* 56 (3), 1084–1097. doi: 10.1021/jm301490d

Wirth, M., Zoete, V., Michielin, O., and Sauer, W. H. B. (2013). SwissBioisostere: A Database of Molecular Replacements for Ligand Design. *Nucleic Acids Res.* 41, D1137–D1143. doi: 10.1093/nar/gks1059

Yamada, Y., Hideka, K., Shiota, S., Kuroda, T., and Tsuchiya, T. (2006). Gene Cloning and Characterization of SdrM, a Chromosomally-Encoded Multidrug Efflux Pump, From Staphylococcus Aureus. *Biol. Pharm. Bull.* 29 (3), 554–556. doi: 10.1248/bpb.29.554

Yoshida, H. (1992). Characterization of the Staphylococcus Aureus norA Gene, Which Confers Resistance to Hydrophilic Quinolones. *Nihon Rinsho* 50 (5), 1042–1048.

Yoshida, H., Bogaki, M., Nakamura, S., Ubukata, K., and Konno, M. (1990). Nucleotide Sequence and Characterization of the Staphylococcus Aureus norA Gene, Which Confers Resistance to Quinolones. *J. Bacteriol.* 172 (12), 6942–6949. doi: 10.1128/jb.172.12.6942-6949.1990

Zhdankin, V. V., Persichini, P. J.III, Zhang, L., Fix, S., and Kiprof, P. (1999). Synthesis and Structure of Benzoboroxoles: Novel Organoboron Heterocycles. *Tetrahedron Lett.* 40 (37), 6705–6708. doi: 10.1016/S0040-4039(99)01303-9

Conflict of Interest: The authors declare that the research was conducted in the absence of any commercial or financial relationships that could be construed as a potential conflict of interest.

Publisher's Note: All claims expressed in this article are solely those of the authors and do not necessarily represent those of their affiliated organizations, or those of the publisher, the editors and the reviewers. Any product that may be evaluated in this article, or claim that may be made by its manufacturer, is not guaranteed or endorsed by the publisher.

Copyright © 2021 Thamilselvan, Sarveswari, Vasudevan, Stanley, Shanmugam, Vairaprakash and Solomon. This is an open-access article distributed under the terms of the Creative Commons Attribution License (CC BY). The use, distribution or reproduction in other forums is permitted, provided the original author(s) and the copyright owner(s) are credited and that the original publication in this journal is cited, in accordance with accepted academic practice. No use, distribution or reproduction is permitted which does not comply with these terms.